PHOTOVOLTAIC EFFICIENCIES IN LATTICE-MATCHED III-V MULTIJUNCTION SOLAR CELLS WITH UNCONVENTIONAL LATTICE PARAMETERS

Emily. C. Warmann[1], Marina S. Leite[1], Harry A. Atwater[1,2]

1. Thomas J. Watson Laboratory of Applied Physics, California Institute of Technology, Pasadena, Ca, United States
2. Kavli Nanosciences Institute, Pasadena, Ca, United States

ABSTRACT

We explore the potential for high efficiency multijunction solar cells that are not lattice matched to currently available single crystal substrates, but are still formed of component subcells that can be lattice matched to one another in the III-V GaInAsP compound semiconductor material system. Using detailed balance calculations, the theoretical efficiency of three and four junction cells with lattice constants in the range from 5.65325 to 5.8687 Å are explored. In this range, a lattice-matched three junction cell with an $In_xAl_{1-x}As$ top subcell has a 56.2% detailed balance efficiency (500 suns). A lattice-matched four junction cell with 54.5% (500 suns) detailed balance efficiency is also identified.

INTRODUCTION

Current III-V multijunction solar cell (MJSC) designs are constrained by the limited range of alloy band gap combinations available for alloys with lattice constant at or near that of single-crystal wafers such as Ge, GaAs or InP. Current champion cells all come from the same family of materials: III-V semiconductor alloys lattice-matched or nearly lattice-matched to GaAs [1-4]. These cell designs employ strategies such as incorporating a germanium bottom cell to allow a lattice-matched three junction cell or incorporating metamorphic, non-lattice-matched subcells with more optimal band gaps to achieve substantial efficiency gains. Nonetheless, these designs are constrained by either lack of flexibility in selecting subcell band gaps (for lattice-matched cells) or by increased defect density for metamorphic designs. Ultimately the limitation comes from the narrow range of band gaps available in the III-V material family at or near the 5.65325 Å (GaAs) lattice constant.

Recent developments have demonstrated the capability to transfer thin, strained epitaxial films from the initial growth substrate to a secondary handle substrate [5,6]. This process can result in defect-free and strain-free single crystal films with lattice constant determined by the unstrained alloy composition. These films can serve as an epitaxial template for subsequent growth at a lattice constant different from any available bulk crystal substrate. Such templates present the opportunity to untether multijunction solar cell designs from the constraint of the limited band gap ranges near the lattice constants of Ge, GaAs or InP.

The III-V material system covers a wide range of band gaps, but not at every lattice constant. The optimal band gaps for a three junction cell are 1.89, 1.28 and 0.84 eV, while an optimal four junction cell has subcell band gaps of 2.06, 1.48, 1.09 and 0.75 eV [7]. As figure 1 shows, the materials with lattice constant near that of GaAs or InP do not have band gaps spanning this range. At lattice constants between these two points the range of band gaps increases, improving the prospects for lattice-matched cell designs. The ability to tailor a growth template to any desired lattice constant promises access to this more optimal range of band gaps.

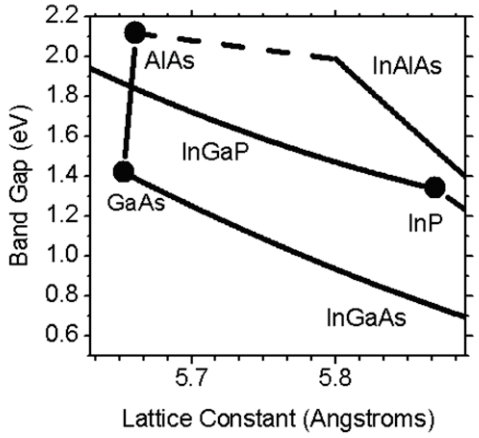

Figure 1. Detail of III-V material family focused on InGaAlAsP materials. The large change in band gap for $In_xGa_{1-x}As$ limits the bottom cell band gap in this region. $In_xAl_{1-x}As$ has an indirect band gap at lattice constants below 5.800Å, indicated by dashed line, and a direct bandgap for larger lattice constants.

The design limitations of the band gap range near 5.65325 Å are illustrated in the performance of the champion multijunction cells in Table 1. Lattice-matched champion GaInP/GaInAs/Ge cells have

measured and theoretical efficiencies shown in the top row. The detailed balance theoretical efficiency for lattice-matched GaInP/GaInAs/Ge cells is lower than that for the champion GaInP/GaInAs/Ge and GaInP/GaInAs/GaInAs metamorphic cells in the second and third rows of Table1. This lower theoretical efficiency is due to the less optimal combination of band gaps in this cell. In particular, the GaAs midcell band gap is higher than optimal, limiting the series current of the structure. Metamorphic champion cells can access a more optimal distribution of subcell bandgaps but this advantage is partially offset by the comparatively high dislocation densities, over $1x10^6/cm^2$ [2], which increase non-radiative recombination and limit cell performance. This compromise between band gap selection and material quality is evident in the similar performance of these different designs.

Materials/Band Gaps	Measured Efficiency	Detailed Balance Efficiency
GaInP/GaInAs/Ge 1.9/1.4/0.7 eV [1]	41.6% 364 suns	50.5% [2]
GaInP/GaInAs/Ge 1.8/1.3/0.7 eV [3]	41.1% 454 suns	54.5% [8]
GaInP/GaInAs/GaInAs 1.8/1.3/0.9 eV [4]	40.8% 326 suns	53.0% [4,8]
SolarJunction [9] Unpublished	43.5% 400 suns	

Table 1. Champion MJSCs with subcell band gaps, record and theoretical efficiencies. The cell in row 1 is lattice matched, while the cells in rows 2 and 3 incorporate metamorphic subcells.

To identify new potential designs for lattice matched MJSCs this analysis calculates the detailed balance efficiency for three and four junction MJSCs with lattice constant between 5.65325 Å (GaAs) and 5.8687 Å (InP). This region of the III-V family contains a wide range of direct band gaps available through ternary and quaternary alloys.

METHODS

Detailed balance calculations provide a way to determine the thermodynamic limiting efficiency of a solar cell design under a range of conditions [9]. These calculations balance the absorbed photons, as determined by the material band gap and incident spectrum, with the collected carriers and radiative recombination (governed by operating voltage) in an ideal cell to determine the maximum conversion efficiency as a function of the cell band gap and operating voltage. For multijunction designs, the problem can be further constrained to require the subcells to operate in electrical series.

This analysis assumed AM1.5 direct illumination under 500x concentration and a cell temperature of 300K. All cells are series-connected. Only band gap combinations that are all present at a particular lattice constant were considered. Specifically, the bottom cell band gap was selected to match that of $In_xGa_{1-x}As$ at each of the lattice constants examined.

For three junction cells, the top and middle cell band gaps were optimized subject to the constraint that the top cell band gap not exceed that of $In_xAl_{1-x}As$ at the particular lattice constant. This alloy has a band gap ranging from 1.59 to 2.12 eV in this region and transitions from a direct to an indirect gap near 5.800 Å. Calculations were performed at a lattice spacing of 0.005 Å and the data linearly interpolated. The results of the calculations for the three junction cells are presented in Figure 2.

Calculations for four junction efficiency assumed a bottom cell band gap equivalent to InGaAs at the desired lattice constant and a top cell band gap equivalent to InAlAs. The two mid cell band gaps were allowed to vary between these values and the overall detailed balance efficiency optimized. The results for the four junction cells are presented in Figure 3.

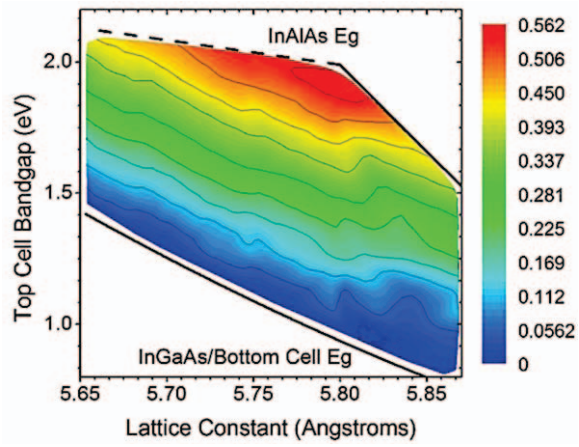

Figure 2. Efficiency plot of three junction cells lattice matched between 5.65325 and 5.8687 Å calculated by detailed balance and shown as a function of top cell bandgap. The bottom cell bandgap is constrained to the InGaAs bandgap and top and middle cells are optimized. The band gap of InAlAs forms an upper limit for the top cell band gap at each lattice constant. The middle cell band gap is optimized for each point and not shown.

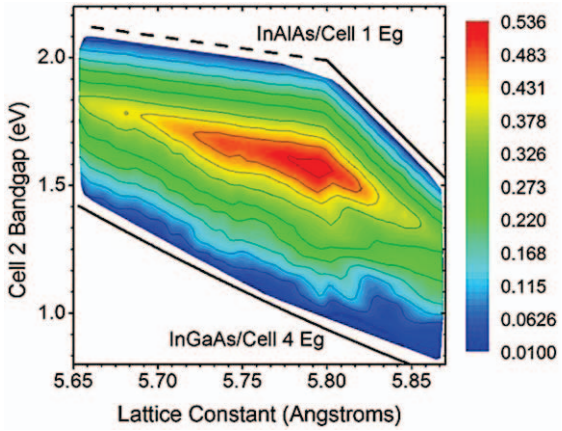

Figure 3. Efficiency plot of four junction cells lattice matched between 5.65325 and 5.8687 Å shown as a function of cell 2 bandgap. The bottom cell is constrained to the InGaAs bandgap and the top cell is constrained to the InAlAs band gap. The second and third cells are optimized at each lattice constant. Cell 3 bandgap is optimized for each point and not shown.

RESULTS

As figures 2 and 3 demonstrate, the efficiency varies dramatically over the region, with the highest potential efficiencies calculated for three and four junction cells lattice-matched between 5.79 and 5.82 Å. The presence of InAlAs as a direct, high bandgap material at lattice constants greater than 5.800 Å allows theoretical efficiencies in excess of 50% for three and four junction designs.

These plots can be divided into two regions where different features govern the efficiency of three and four junction cell designs. In the region from 5.800 to 5.8687 Å, the band gap of InGaAs varies from 0.94 to 0.77 eV, close to the optimal three and four junction bottom cell band gaps. The primary constraint on efficiency in this region comes from the top cell band gap limit set by InAlAs, which varies from 2.0 to 1.59 eV. At higher lattice constants, the InAlAs band gap is lower than optimal for three and four junction cells. At 5.8687 Å the efficiency is 40.7% for three junction and 36% for four junction cells. As the lattice constant decreases, these efficiencies increase to 56.2% for three junction and 54.5% for four junction cells at 5.800 Å. The three junction efficiency is only slightly lower at 5.810 Å, 55.9%.

At lattice constants below 5.800 Å the band gap of InAlAs ranges from 2.12 to 2.0 eV and poses neither current nor voltage constraint for the cells below. In this region the band gap of InGaAs varies from 1.424 to 0.94 eV, which is everywhere too high to be an optimal bottom cell for three or four junction designs and presents an increasingly severe current limit on the designs. It is also important to note that InAlAs has an indirect band gap in this region, making it an impractical material for use in MJSCs. The analysis does not take into account the increased thickness an indirect band gap material would require, but this must be considered when identifying potential cell designs.

Figure 4 shows the optimized band gaps and efficiencies for three and four junction lattice matched cells. These band gaps correspond to the highest detailed balance efficiency possible for lattice matched cells at each lattice constant between 5.65325 and 5.8687 Å. Interestingly, the most efficient three junction cells from 5.800 and 5.810 Å do not incorporate top cells with the band gap of InAlAs at those lattice constants, rather they have top cells of approximately 1.9 eV band gap. This suggests that there is no benefit to further decreasing the lattice constant to improve the top cell band gap for three junction cells. Indeed, three junction cells at smaller lattice constants have lower efficiency due to the increasing band gap of InGaAs, which serves to limit the cell current. For lattice constants less than 5.73 Å, this current limit shifts the top cell optimal band gap back up to the limit imposed by InAlAs and the efficiency drops off rapidly. The maximum efficiency four junction cell is 54.5% at 5.798 Å. This is constrained by limits on both the top and bottom cell band gaps, resulting in a lower efficiency than can be achieved with three junctions.

As figure 4 shows, the four junction design is less efficient than a three junction design everywhere in this region. This counterintuitive result springs from the non-optimal top and bottom cell band gaps in this region, as caused by the InGaAs and InAlAs constraints. The ideal four junction design has a bottom cell band gap of 0.72 eV. This is lower than the band gap of InGaAs everywhere in this region of lattice constants, and consequently the bottom cell band gap limits the total number of photons available to the cell. This limitation is minimal near 5.8687 Å but grows increasingly severe as the lattice constant decreases and the bottom cell band gap varies from 0.77 to 1.424 eV. Specifically, the number of photons with sufficient energy to be absorbed by the cell drops by 63%. The ideal four junction top cell band gap is 2 eV, which is available at lattice constants below 5.800 Å, however this is the region with the most significant bottom cell current limits. In contrast, in the region from 5.800 to 5.8687 Å the InAlAs band gap decreases sharply. Here the top cell creates the current limits, which result in the steep drop in efficiency evident in figure 4 (c). The current limits created by the constraints on the top and bottom cell band gaps combine with the voltage limit created by the top cell band gap limit to negate any benefit from the additional spectral division gained by moving from three cells to four.

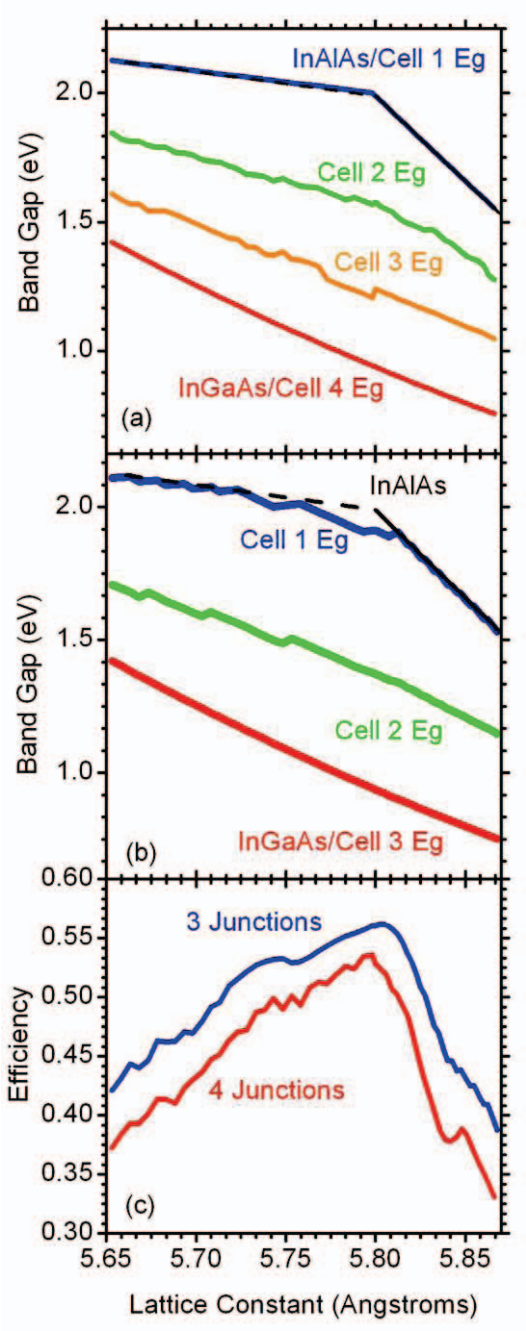

Figure 4. Optimized band gaps for lattice matched (a) four and (b) three junction cells and (c) their detailed balance efficiency vs lattice constant for the region from 5.65325 (GaAs) and 5.8687 (InP) Å

CONCLUSIONS

Detailed balance calculations identify a 56.2% efficient three junction MJSC that is lattice-matched at 5.805 Å. This improves on current designs and motivates the fabrication of a 5.805 Å template for growth of these three junction cells. Analysis of four junction designs indicates there is insufficient range of band gaps in this region, resulting in current limited designs that are less efficient than three junction cells.

ACKNOWLEDGEMENTS

The authors acknowledge financial support from the Department of Energy – Solar Energy Technology Program under Grant No. DE-FG36-08GO18071. We also acknowledge M. Archer for developing the detailed balance Matlab code.

REFERENCES

[1] R. R. King, *et al*., "Band-gap Engineered Architectures for High-Efficiency Multijunction Concentrator Solar Cells," in *Proceedings of the 24th European Photovoltaic Solar Energy Conference*, Hamburg, Germany, 2009.

[2] R. King, et al., "40% Efficient Metamorphic GaInP/GaInAs/Ge Multijunction Solar Cells," *Applied Physics Letters* 2007; 90: 183516.

[3] W. Guter, et al., "Current-Matched Triple-Junction Solar Cell Reaching 41.1% Conversion Efficiency Under Concentrated Sunlight," *Appl. Phys. Lett.* **94**(22), 2009, p. 223504.

[4] J. F. Geisz, et al., "40.8% Efficient Inverted Triple-Junction Solar Cell with Two Independently Metamorphic Junctions," *Appl. Phys. Lett*. **93**(12), 2008, p. 123505.

[5] M. S. Leite, et al., "Wafer-Scale Strain Engineering of Ultra-Thin Semiconductor Crystalline Layers for Epitaxial Growth," *in review*, 2011.

[6] H. Fang, et al., "Strain Engineering of Epitaxially Transferred, Ultrathin Layers of III-V Semiconductor on Insulators," *Appl. Phys. Lett.* **98**(1) 2011, p.12111.

[7] I. Tobias and A. Luque, "Ideal Efficiency of Monolithic, Series-Connected Multijunction Solar Cells," *Progress in Photovoltaics* **10**, 2002, pp. 323-329.

[8] S. Kurtz, D. Myers, W. E. McMahon, J. Geisz, and M. Steiner, "A Comparison of Theoretical Efficiencies of Multi-Junction Concentrator Solar Cells," *Progress in Photovoltaics* **16**(6), 2008, pp. 537–546.

[9] S. Olson (2011, Apr. 14). “NREL Confirms World-Record 43.5% Efficiency on Solar Junction’s CPV Cell.” Retrieved June 6, 2011 from http://www.pv-tech.org/news/nrel_confirms)world_record_43.5_efficiency_on_solar_junctions_cpv_cell

[10] C. H. Henry, “Limiting Efficiencies of Ideal Single and Multiple Energy Gap Terrestrial Solar Cells,” *J. Appl. Phys.* **51**(8), 1980, pp. 4494–4500.